



Single electron tracks in water vapour for energies below 100 eV

A. Muñoz^a, F. Blanco^b, G. Garcia^{c,d,*}, P.A. Thorn^e, M.J. Brunger^e,
J.P. Sullivan^d, S.J. Buckman^d

^a Centro de Investigaciones Energéticas Medioambientales y Tecnológicas (CIEMAT), Avenida Complutense 22, 28040 Madrid, Spain

^b Departamento de Física Atómica, Molecular y Nuclear, Universidad Complutense de Madrid, Avenida Complutense sn, 28040 Madrid, Spain

^c Instituto de Matemáticas y Física Fundamental, Consejo Superior de Investigaciones Científicas, Serrano 113-bis, 28006 Madrid, Spain

^d ARC Centre for Antimatter-Matter Studies, RSPHysSE, Australian National University College of Science, Canberra, ACT 0200, Australia

^e ARC Centre for Antimatter-Matter Studies, SoCPES, Flinders University, G.P.O. Box 2100, Adelaide, South Australia 5001, Australia

ARTICLE INFO

Article history:

Received 31 March 2008

Received in revised form 30 April 2008

Accepted 30 April 2008

Available online 7 May 2008

Keywords:

Electron track simulation

Electron cross sections in water

ABSTRACT

A new method to simulate single electron tracks, from 0 to 100 eV, in water vapour is described. In this method we employ as input parameters the experimental and theoretical electron interaction cross sections and also relevant experimental energy loss distribution functions. Most of the open inelastic processes (ionization, neutral dissociation, electronic, vibrational and rotational excitation) are considered in this energy range, as well as the elastic scattering channel. Angular distributions of the scattered electrons have been related to the momentum transfer, indicating some analytical regularity which allows us to greatly simplify the computational procedures. The determined simulated track structure has then been used to derive energy deposition profiles, and thus the induced radiation damage.

© 2008 Elsevier B.V. All rights reserved.

1. Introduction

Water is one of the most relevant molecular components in living organisms. It therefore has been the subject of a large number of experimental and theoretical studies, in order to determine collisional data for photons, electrons and other particles related to radiation physics and chemistry. In particular electrons, being the main resultant secondary particle, are present in most of these studies. Comprehensive reviews on electron interactions with water, over a broad energy range, have been recently published [1,2]. However, due to inherent properties of the water molecule such as its strong permanent dipole moment, important discrepancies between theory and experiment remain below 10 eV. This is true even for essential parameters like the total scattering cross section. Above 10 eV, remarkable contradictions between the measured ionization cross sections and the latest calculation [3] also remain as an example for these discrepancies. Although in the last few years an important effort has been made to develop energy deposition models, to be used in biomedical applications of radiation [4–6], this fundamental data inconsistency is affecting the reliability of those models. In this study we therefore present a critical review of existing experimental and theoretical data below 100 eV.

By combining previous measurements with our model potential calculations, we propose a partition of elastic and inelastic channel cross sections which is consistent with the most accurate total cross section measurements and representative low energy elastic as well as rotational excitation calculations. The complete set of differential and integral cross section data derived from this analysis, is subsequently employed to simulate single electron tracks in water vapour by using a step by step Monte Carlo simulation procedure [7,8]. Track structure given by this simulation provides relevant information of biomedical interest, such as energy deposition maps and radiation damage in terms of molecular alterations.

2. Cross sectional data

2.1. Total electron scattering cross sections

The difficulties which are encountered in measuring total electron scattering cross sections for low energy electrons in water have been discussed elsewhere [3]. Essentially this arises because elastic and rotational excitation cross sections increase rapidly as the electron energy decreases. In particular their differential cross section values are strongly peaked in the forward scattering angle direction. In addition, as the energy gap between rotational levels is only a few meV [9], extremely good energy and angular resolution is required to distinguish between scattered and non-scattered electrons in typical total cross section transmission beam experiments. Early examples of these measurements [10,11] did not achieve those con-

* Corresponding author at: Instituto de Matemáticas y Física Fundamental, Consejo Superior de Investigaciones Científicas, Serrano 113-bis, 28006 Madrid, Spain.
E-mail address: g.garcia@imaff.cfmac.csic.es (G. Garcia).

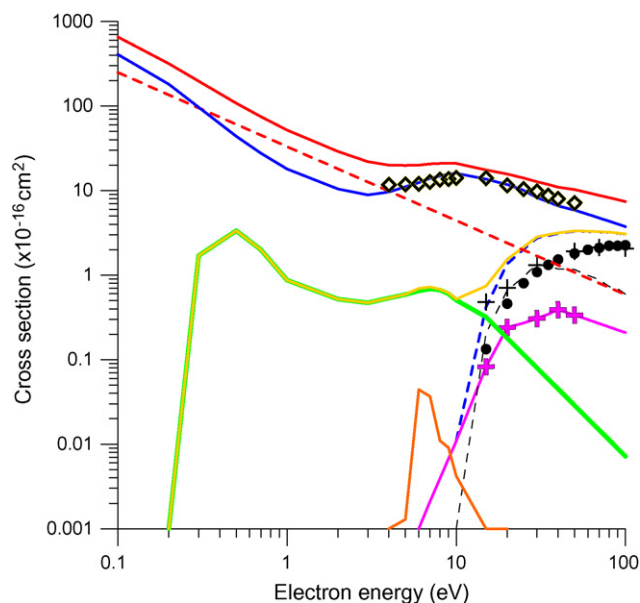


Fig. 1. Integral cross sections for electron scattering in H₂O (see text for data sources): (◇) Cho et al. [31]; (—) total electron scattering (reference values); (—) integral elastic; (---) rotational excitation; (—) integral inelastic (excluding rotational excitation); (---) integral inelastic (model potential calculations); (—) vibrational excitation; (—) electron attachment; (●) ionization; (+) experimental electronic excitation; (■) extrapolated electronic excitation; (---) remainder inelastic channels (neutral dissociation); (+) experimental neutral fragmentation.

ditions, so that the observed total cross sections tended to be much lower than the calculated values [12]. However recent measurements from Jones and co-workers [13], using an energy resolution better than 2 meV, gave results only slightly higher than the previous experiments but still far away from the theoretical predictions. Obviously those new results still require a correction for the angular acceptance of the detector, but all else seems to indicate that other factors need to be taken into consideration for a proper comparison between the theoretical and experimental data. As one example of those additional factors we note that the experimental molecular targets are not actually in the ground state, as assumed in the calculations. In fact they present a rotational level distribution, according to their temperature, and therefore direct comparison between theory and experiment is not strictly viable. As the systems we are going to simulate are closer to the experimental conditions, than to the ideal situation of the calculations, we are thus employing the experimental values as our reference for the total cross section data. With respect to the best experimental energy and angular resolution, relative to the incident energy and from data available in the literature, we chose three set of measurements to determine our reference values: the results of Jones and co-workers [13] for the lower energy domain (0.03–5.4 eV), those of Szmytkowski [11] for low and intermediate energies (5–80 eV), and our recent measurements [3] for higher energies (50–100 eV). Total electron scattering cross sections for incident energies from 0.03 to 100 eV, derived from these experimental data, are hence shown in Fig. 1. Taking into account the quoted experimental errors and the statistical deviations in the overlapping energy intervals, the estimated uncertainties for these data remain within 6%.

2.2. Ionization cross sections

Ionization of water molecules by electron impact has been studied since the early years [14–17] of scattering measurements. Discrepancies due to systematic errors in those measurements

were, however, overcome by the accurate measurements of Straub et al. [18]. Although recent calculations [19] showed discrepancies with those experimental results, our current measurements from 50 eV impact energy corroborate the data in Ref. [18]. We therefore use the experimental ionization cross sections of [18] from threshold to 100 eV, as shown in Fig. 1, in our simulations. Note the uncertainty on these data is $\sim 7\%$ which is in accord with our confirmation measurements [3].

2.3. Electronic excitation cross sections

Integral electronic excitation cross sections have been derived from the electron energy loss analysis carried out by Thorn and Brunger [20], from 15 to 50 eV. Differential cross sections for individual and unresolved excited states, accessible for each incident energy, have been integrated and added together. As shown in Fig. 1, those summed experimental values have been extrapolated up to 100 eV and down to the threshold excitation energy by assuming a simple double logarithmic energy dependence of the cross sections with energy. Considering the quoted experimental errors and errors associated with the extrapolation procedures, an accuracy of 20–40% can be assigned to these values.

2.4. Vibrational excitation and electron attachment

Values recommended by Itikawa and Mason [1] have been considered for these two inelastic channels. Vibrational excitation data are based on available experiments [10,21–23], but giving more weight to the most recent results [22,23]. Concerning dissociative electron attachment to water molecules, no recent measurements have been found beyond the recommended experimental data from [24].

2.5. Remaining scattering channels

As we have already mentioned, our model potential procedure [25–27] has been used to calculate differential and integral elastic scattering cross sections, as well as integral inelastic scattering of electrons in H₂O from 1 to 100 eV. In a similar manner to that proposed in [3], the ratio of the inelastic to total cross sections, given by the calculations, can be used to derive the remaining integral inelastic cross sections from the reference values we determined in Section 2.1. Since that model approach considers inelastic scattering as electron–electron interactions, in those integral inelastic cross sections both vibrational excitation and electron attachment are excluded. Therefore, by subtracting the ionization and the electronic excitation cross sections from the model integral inelastic cross sections, the resulting data represent the remaining inelastic channels which should be related to neutral dissociation. The reliability of this procedure can be subsequently checked, by comparing this “remaining” cross section with the available neutral dissociation cross section measurements given in [28,29]. As shown in Fig. 1, those neutral dissociation cross section values generally agree with our corresponding “remaining” cross section although they do tend to be a little higher at low energies. This tendency can be explained by noting that some of the neutral fragments observed in [28,29] come from electronically excited states, which we have already included in the electronic excitation cross sections of Section 2.3. By adding all the inelastic channels considered in 1.2–1.5, total inelastic cross sections can be obtained and their consistency with measurements and calculations is demonstrated in the above discussion.

2.6. Elastic scattering and rotational excitation

From the experimental point of view, it is difficult to discriminate against rotational excitation of molecules, particularly for molecules with an important permanent dipole moment, as is the case with water, from the elastic processes. In addition, at small scattering angles it is difficult to distinguish between unscattered and elastically scattered electrons. To some extent, depending on the angular and energy resolution of the experiment, most elastic measurements include some contamination from these effects. The procedure we are thus proposing here, to determine elastic scattering cross sections and rotational excitation from our cross section database, is the following:

By subtracting the total inelastic cross sections derived in Section 2.5 from our reference total cross section of Section 2.1, we obtain a sum of the elastic and the rotational excitation cross sections. The rotational excitation of a species with a permanent dipole, by electron impact, can be easily calculated in the Born approximation, with formulae as given in [30]. As shown in Fig. 1, the energy dependence of the integral rotational cross section calculated with these formulae follow a straight line on a logarithmic plot. As expected, at 50 eV incident energy our calculated integral elastic cross sections, which exclude rotational excitations, and the experimental values of Cho et al. [31], for which rotational contamination should be negligible at this energy, show agreement to within 10%. By fitting the amplitude of this straight line, to obtain at this energy an elastic cross section value in agreement with those both calculated and measured, we could separate the rotational excitation process cross sections from those for elastic scattering over the entire considered energy range (0–100 eV). The accuracy of this procedure is linked to the suitability of the Born approximation and is therefore difficult to quantify. However, the self-consistency between the theoretical and experimental total cross section data suggests that uncertainties related to the average rotational excitation cross section should be less than 15%. Integral elastic scattering cross sections obtained with this procedure are also shown in Fig. 1. As can be seen from this figure, these elastic values agree with the measurement given in [31] (from 4 eV) and give results consistent with our reference TCS values.

3. Angular distribution functions

In previous studies [7,8] we demonstrated how the differential cross sections, calculated with the above mentioned model potential procedure, can be used to simulate the angular distribution of electrons after a collision process. In this case we are introducing an improvement to that approach by using these differential values as a function of the momentum transfer. For elastic processes, by neglecting the recoil velocity of the molecular target, momentum transfer implies a simple change in the direction of the scattered electron with respect to the incident one. In Fig. 2, elastic differential cross sections as a function of the momentum transfer are shown for the present calculation and for the experimental data of Cho et al. [31], at different energies. As can be seen, they all agree well in shape thereby providing a straightforward dependence which simplifies the way of introducing the data in the simulation procedure. Moreover, considering inelastic collisions we note that their momentum transfer includes the momentum magnitude decrease corresponding to the energy transferred to the target. Taking this energy from the experimental energy loss spectra, Fig. 3 represents the momentum transfer dependence for the differential cross sections of the elastic and inelastic processes at 40 eV, derived from the energy loss spectra from [20], at three different scattering angles, 10°, 50° and 80°, respectively. Also shown in Fig. 3 are least squares fits to these respective elastic and inelastic data, in order

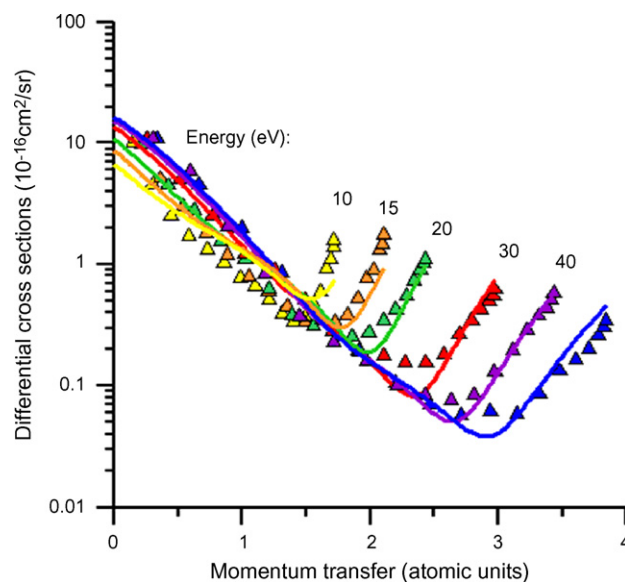


Fig. 2. Elastic differential cross sections for electron scattering from H₂O as a function of the momentum transfer: (—) present calculations; (Δ) measurements from [31].

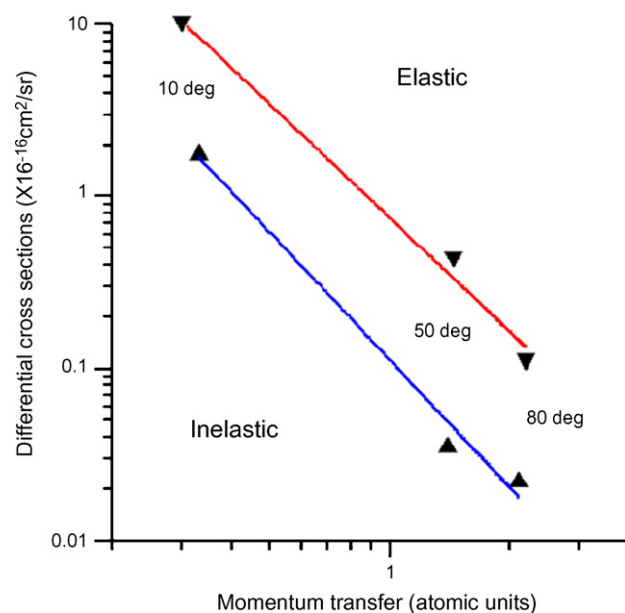


Fig. 3. Comparison of elastic and inelastic differential cross sections, derived from the experimental energy loss spectra of [20], as a function of the momentum transfer. The incident electron energy is 40 eV in each case.

to assist the reader to visualize how similar the shapes of these cross section dependencies are. Given that the behaviour in Fig. 4, at 40 eV, is representative for all incident energies from 10 to 100 eV, we can assume that having introduced the appropriate momentum transfer, including the energy loss for the inelastic collisions, the inelastic angular distribution of the scattered electrons can be simply determined from that for the elastic case. This further simplifies the assimilation of the inelastic data into the simulation code.

4. Energy loss distribution functions

As has already been mentioned, the energy distribution functions assumed in this study for the scattered electrons are based on

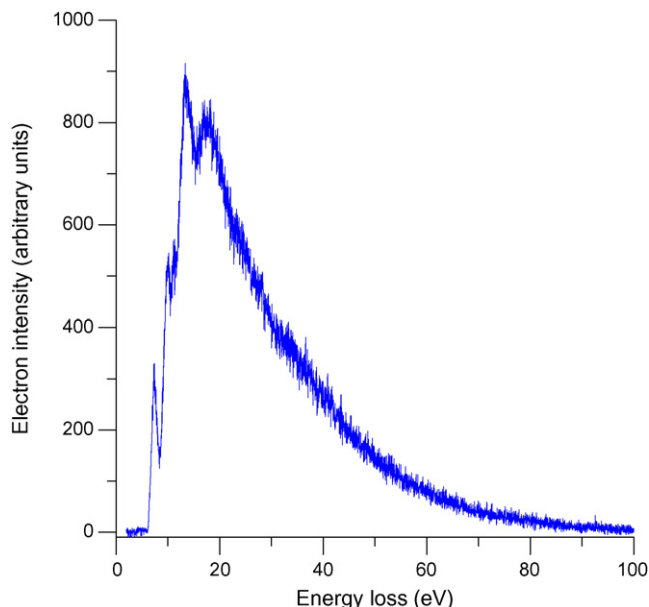


Fig. 4. Average energy loss distribution function for high energy electrons in H₂O. This applies for incident electrons with energies in the range 40–100 eV.

experimental energy loss spectra. We have recently shown [3] that, for high enough energies, a reasonably unique energy loss distribution function can be achieved by averaging energy loss spectra over those for different energies and different scattering angles. This average energy loss function is shown in Fig. 4 and it will be used here to determine the energy transferred by electrons in single collisions when their incident energy is between 40 and 100 eV. Below 40 eV, as larger scattering angles tend to be more important, the angular range has been divided into four regions delineated by 10°, 50° and 80°. By averaging the energy loss for each angular region, the accuracy of the energy loss distribution function for the low energy electrons can be maintained to better than 10%. In Fig. 5 the energy loss spectra for 40 eV incident electrons at the relevant

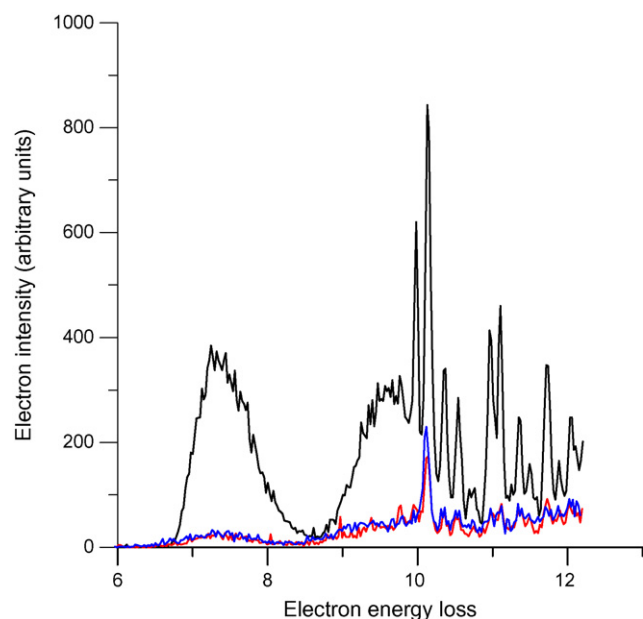


Fig. 5. Energy loss spectra of 40 eV electrons in H₂O, as a function of the scattering angle: (—) 10°; (—) 50°; (—) 80°. Data are from reference [20].

different scattering angles is plotted, showing the angular dependence of the scattered intensity. It is from those data that the low energy (<40 eV) energy loss distribution function is calculated.

5. Modeling electron tracks

The cross section data and energy loss distribution functions described above, have been integrated in a Monte Carlo code to simulate single electron tracks. Technical details of that code have been published in previous papers [7,8], so we will give here only a brief description. Total cross sections define the mean free path and, therefore, when a collision event takes place. From the integral cross section data the program next decides if the collision is elastic or inelastic. In an elastic collision no energy deposition occurs and the scattering angle is decided from the angular distribution functions, as a function of the incident energy and the momentum transfer. However, if the collision is inelastic, the energy loss distribution function determines the amount of energy transferred to the medium and the momentum transfer. From the probability distribution of the different accessible inelastic channels, the program now decides which type of inelastic process has taken place and finally the direction of the inelastically scattered electron. Note that when an ionization collision occurs, this implies that a secondary electron is automatically generated. The energy distribution of the secondary electrons is given by the energy loss distribution function, by assuming that the energy deposited in ionizing events is just the ionization energy and the rest is entirely transmitted to the ejected electron. The angular distribution of the secondary electrons is derived from the momentum transferred by the incident electron in combination with the momentum conservation law. Figs. 6 and 7 represent typical electron tracks, showing the energy loss that occurs in single collisions and the type of process which is taking place, respectively. As shown in Fig. 8, this track structure subsequently allows a detailed evaluation of the energy deposition as a function of the electron penetration in the medium.

We have not found any other available simulation code results for electron energies below 100 eV, to compare with the single track structure given in this study. Concerning other potentially available quantities, such as the stopping power, to derive energy deposition profiles to compare with the present, important inconsistencies of

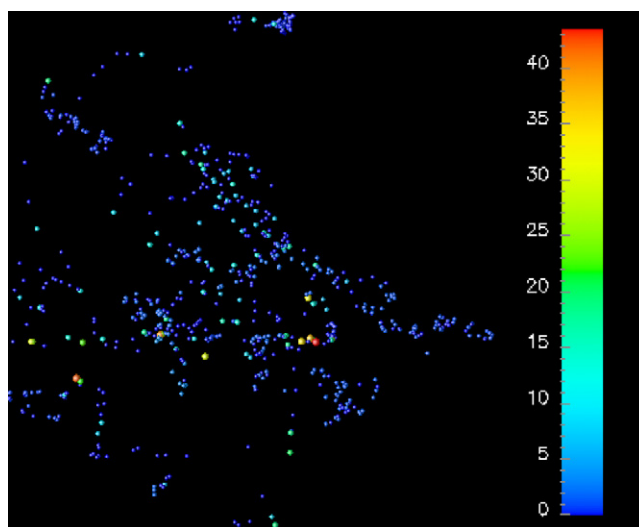


Fig. 6. Single tracks corresponding to five 100 eV electrons in 500 mTorr of water vapour. Colour scale indicates the energy loss in each collision process from red (more than 40 eV) to deep blue (0 eV which corresponds to elastic scattering).

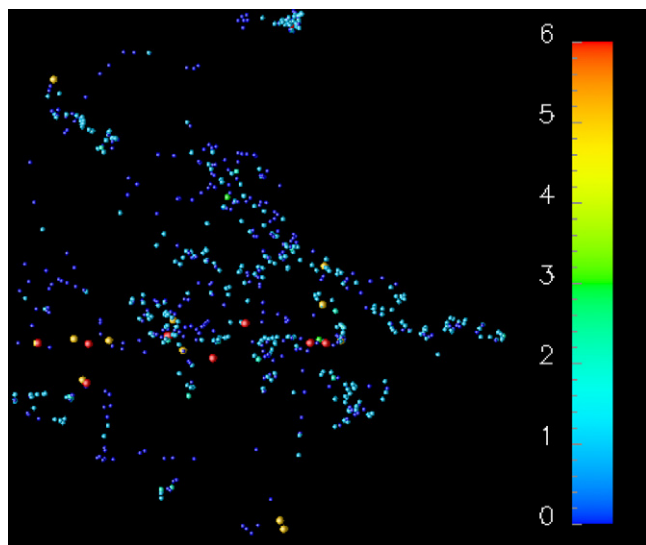


Fig. 7. Same electron tracks as in Fig. 6 but now indicating with colour codes the type of collision process as follows: 0, elastic scattering; 1, rotational excitation; 2, vibrational excitation; 3, electronic excitation; 4, electron attachment; 5, neutral dissociation; 6, ionization.

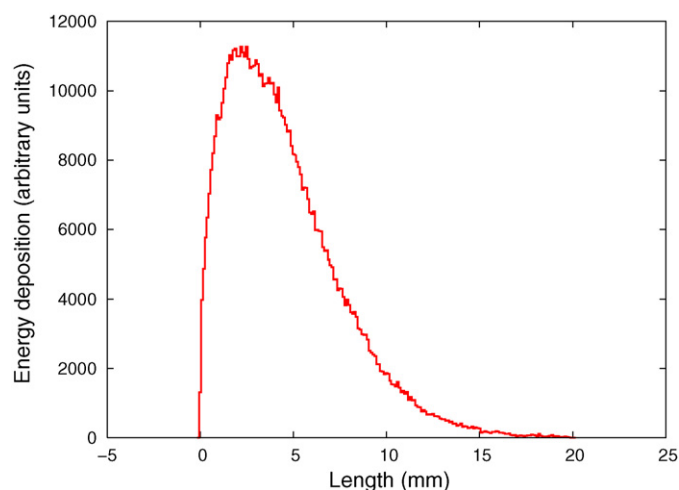


Fig. 8. Energy deposition of 100 eV electrons in 500 mTorr of water vapour, as a function of length.

these parameters found in previous studies (see e.g., [3]) make it not a recommended course of action. At this point, future experimental validation of the present results would be desirable and more profitable.

6. Conclusions

A complete set of differential and integral electron scattering cross section data for H₂O, based on our previous measurements, calculations and some data available in the literature, has been provided. The consistency of these data for all elastic and inelastic channels, including rotational excitation, has been established.

These data were subsequently used as input parameters for a Monte Carlo simulation code, which provides information on energy deposition and induced damage at the molecular level. Since no previous results from simulation codes, operating at the energy range considered here, have been found an experimental validation of the present results is required.

Acknowledgements

This study has been partially supported by the following research projects and institutions: Ministerio de Educación y Ciencia (Plan Nacional de Física, Project FIS2006-00702), Consejo de Seguridad Nuclear (CSN), European Science Foundation (COST Action P9 and EIPAM Project), Acciones Integradas Hispano-Portuguesas (Project HP2006-0042). We acknowledge N. C. Jones and D. Field for providing their unpublished cross section data. The Australian participants acknowledge support from the Australian Research Council under its Centres of Excellence Programme. We also acknowledge support under the DEST/ISL programme, that enabled one of us (GG) to visit Australia.

References

- [1] Y. Itikawa, N.J. Mason, *J. Phys. Chem. Ref. Data* 34 (2005) 1.
- [2] Y. Itikawa (Ed.), *Landolt-Börnstein: Numerical Data and Functional Relationships in Science and Technology, Group I, Volume 17, Subvolume C, Photon and Electron Interactions with Atoms, Molecules and Ions*, Springer, Berlin/Heidelberg, 2003.
- [3] A. Muñoz, J.C. Oller, F. Blanco, J.D. Gorfinkiel, P. Limao-Vieira, G. Garcia, *Phys. Rev. A* 76 (2007) 052707.
- [4] C. Champion, *Phys. Med. Biol.* 48 (2003) 2147.
- [5] D. Emfietzoglou, F.A. Cucinotta, H. Nikjoo, *Radiat. Res.* 164 (2005) 202.
- [6] D. Emfietzoglou, H. Nikjoo, *Radiat. Res.* 167 (2007) 110.
- [7] A. Muñoz, A. Williard, J.M. Perez, F. Blanco, G. Garcia, *J. Appl. Phys.* 95 (2004) 5865.
- [8] A. Muñoz, J.M. Perez, G. Garcia, F. Blanco, *Nucl. Instrum. Meth. A* 536 (2005) 176.
- [9] H.M. Randall, D.M. Dennison, N. Ginsburg, L.R. Weber, *Phys. Rev.* 52 (1937) 160.
- [10] G. Seng, F. Linder, *J. Phys. B* 9 (1976) 2539.
- [11] C. Szymkowski, *Chem. Phys. Lett.* 136 (1987) 363.
- [12] A. Faure, J.D. Gorfinkiel, J. Tennyson, *J. Phys. B* 37 (2004) 801.
- [13] R. Čurík, J.P. Ziesel, N.C. Jones, T.A. Field, D. Field, *Phys. Rev. Lett.* 97 (2006) 123202 (And private communication).
- [14] B.L. Schraam, F.J. de Heer, M.J. Van der Wiel, J. Kistemaker, *Physica* 31 (1965) 94.
- [15] D. Rapp, P. Englander-Golden, *J. Chem. Phys.* 43 (1965) 1464.
- [16] R.R. Gorugantou, W.G. Wilson, R.A. Bonham, *Phys. Rev. A* 35 (1987) 540.
- [17] C.B. Opal, E.C. Beaty, W.K. Peterson, *At. Data* 4 (1972) 209.
- [18] H.C. Straub, P. Renault, B.G. Lindsay, K.A. Smith, R.F. Stebbings, *Phys. Rev. A* 54 (1996) 2146.
- [19] M. Vinodkumar, K.N. Joshipura, C. Limbachiya, N.J. Mason, *Phys. Rev. A* 74 (2006) 022721.
- [20] P.A. Thorn, M.J. Brunger, P.J.O. Teubner, N. Diakomichalis, T. Maddern, M.A. Bolorizadeh, W.R. Newell, H. Kato, M. Hoshino, H. Tanaka, H. Cho, Y.-K. Kim, *J. Chem. Phys.* 126 (2007) 064306; M.J. Brunger, P.A. Thorn, L. Campbell, N. Diakomichalis, H. Kato, H. Kawahara, M. Hoshino, H. Tanaka, Y.-K. Kim, *Int. J. Mass. Spectrom* 271 (2008) 80; P.A. Thorn, M.J. Brunger, H. Kato, M. Hoshino, H. Tanaka, *J. Phys. B* 40 (2007).
- [21] T.W. Shyn, S.Y. Cho, T.E. Cravens, *Phys. Rev. A* 38 (1988) 678.
- [22] A. El-Zein, M.J. Brunger, W.R. Newell, *J. Phys. B* 33 (2000) 5033.
- [23] A. El-Zein, M.J. Brunger, W.R. Newell, *Chem. Phys. Lett.* 319 (2000) 701.
- [24] C.E. Melton, *J. Chem. Phys.* 57 (1972) 4218.
- [25] F. Blanco, G. García, *Phys. Rev. A* 67 (2003) 022701.
- [26] F. Blanco, G. García, *Phys. Lett. A* 317 (2003) 458.
- [27] F. Blanco, G. García, *Phys. Lett. A* 330 (2004) 230.
- [28] W. Kedzierski, J. Derbyshire, C. Malone, J.W. McConkey, *J. Phys. B* 31 (1998) 5361.
- [29] T. Harb, W. Kedzierski, J.W. McConkey, *J. Chem. Phys.* 115 (2001) 5507.
- [30] L.A. Collins, D.W. Norcross, *Phys. Rev. A* 18 (1978) 467.
- [31] H. Cho, Y.S. Park, H. Tanaka, S.J. Buckman, *J. Phys. B* 37 (2004) 625.